

Nucleophilic Addition to Olefins. 12.¹ Solvent-Induced Change in the Rate-Limiting Step of the Hydrolysis of Benzylidenemalononitrile in Acidic Me₂SO-Water Solution

Claude F. Bernasconi,* Anastassia Kanavarioti, and Robert B. Killion, Jr.

Contribution from the Thimann Laboratories of the University of California, Santa Cruz, California 95064. Received September 24, 1984

Abstract: A kinetic study of the reversible, four-step hydrolysis of benzylidenemalononitrile (BMN) to form benzaldehyde and malononitrile in water and Me₂SO-water mixtures (50%, 60%, and 70% Me₂SO (v/v)) is reported. At pH ≤ 2 the breakdown of the neutral tetrahedral intermediate, PhCH(OH)CH(CN)₂ (T^o_{OH}, Scheme I, *k*₃₄^{H₂O}), is rate limiting in all solvents. Above pH 2 the breakdown of the anionic intermediate, PhCH(O⁻)CH(CN)₂ (T⁻_O, Scheme I, *k*₄), is rate limiting in water, while in the presence of Me₂SO oxygen deprotonation of T^o_{OH} (*k*₃^B) becomes partially rate limiting at low buffer concentrations. A detailed kinetic analysis, coupled with a few assumptions about rates of diffusion-controlled proton transfers, allows one to estimate the rate and equilibrium constants of all kinetically important steps. This analysis shows that the solvent-induced change in the rate-limiting step is caused by an enhanced rate of breakdown of T⁻_O (*k*₄) in the Me₂SO-containing solvents. This rate enhancement can be understood in terms of an increased "push" by the less solvated anionic oxygen of T⁻_O. This increased "push" is somewhat attenuated by a reduced "pull" which arises from the slight destabilization of CH(CN)₂⁻ in the Me₂SO-containing solvents. On a more quantitative level the equilibrium constant, *K*₄, for the breakdown of T⁻_O into benzaldehyde and CH(CN)₂⁻ correlates remarkably well with the estimated solvent activity coefficients of T⁻_O (^Wγ^D_{T⁻_O) and CH(CN)₂⁻ (^Wγ^D_{CH(CN)₂⁻). A correlation of the solvent effect on the rate constant, *k*₄, of the breakdown of T⁻_O with the same solvent activity coefficients suggests that the sensitivity of *k*₄ to ^Wγ^D_{CH(CN)₂⁻} (*β*_{18,sol} ≈ 0.78 ± 0.10) is greater than its sensitivity to ^Wγ^D_{T⁻_O} (*β*_{N,sol} ≈ 0.57 ± 0.05). This "imbalance" is attributed to a rate-retarding effect which arises from early desolvation of the oxyanion in the transition state, an effect which is magnified in the less aqueous solvents. The direct breakdown of T^o_{OH} into benzaldehyde and malononitrile (*k*₃₄^{H₂O}) probably occurs by a mechanism in which C-C bond cleavage is concerted with the removal of the OH proton by the solvent. Suggestive, though inconclusive, evidence is presented in favor of a transition state (2) in which oxygen deprotonation is coupled with protonation of the departing carbanion.}}

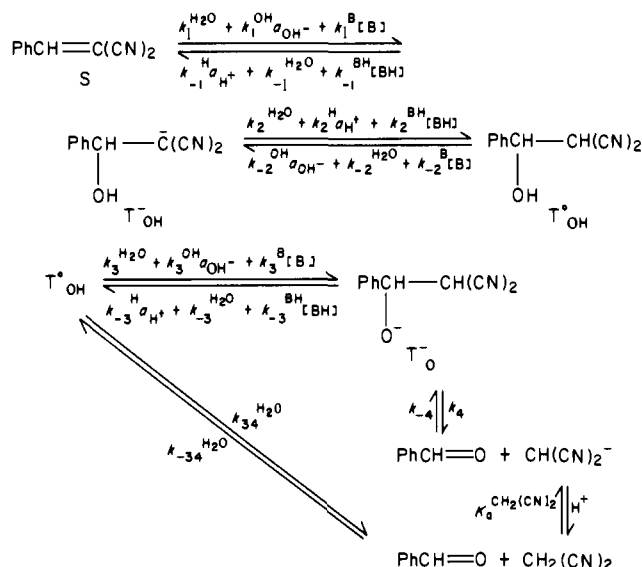
The reversible hydrolysis of benzylidenemalononitrile (BMN) proceeds by the mechanism shown in Scheme I,¹ a mechanism which is typical for the hydrolysis of activated olefins in general.²⁻⁶ In aqueous solution at 25 °C the following steps are rate limiting in various pH ranges:¹ *k*₃₄^{H₂O} at pH ≤ 0.3; *k*₄ at pH 0.3-5.0; *k*₁^{H₂O} at pH 5.0-8.0; *k*₁^{OH} at pH 8.0-12.8.

In this and a subsequent paper⁷ we wish to examine the effect of adding increasing amounts of dimethyl sulfoxide to the solvent on the rate constants of the various steps shown in Scheme I. The present paper deals with the reaction in acidic solution and the subsequent paper with the reaction in basic solution.

The addition of dimethyl sulfoxide to the solvent leads to a significant destabilization of T⁻_O because of reduced hydrogen-bonding solvation.⁸ This effect will increase the thermodynamic driving force of the breakdown of T⁻_O into benzaldehyde and CH(CN)₂⁻ and should increase *k*₄. This raises the question as to whether the increase in *k*₄ (4.66 × 10⁴ s⁻¹ in water at 25 °C)¹ is sufficient to produce a change in rate-limiting step from rate-limiting *k*₄ (*k*₄ << *k*₋₃^{H₂O} + *k*₋₃^H*a*_{H⁺} + *k*₋₃^{BH}[BH]) in water to (partially) rate-limiting oxygen deprotonation of T^o_{OH} (*k*₄ > (>>) *k*₋₃^{H₂O} + *k*₋₃^H*a*_{H⁺} + *k*₋₃^{BH}[BH]) in Me₂SO-water.

We now report that in 50%, 60%, and 70% aqueous dimethyl sulfoxide oxygen deprotonation of T^o_{OH} indeed becomes (partially) rate limiting. We also show how insights about the transition-state structure for step *k*₄ can be obtained from the solvent dependence of *k*₄ compared to that of *K*₄.

Scheme I



Results

In general the same experimental problems were encountered and the same procedures were used as those reported for our study in water,¹ except for the following three minor differences. (1) Because of strong solvent absorption at 250 nm (λ_{max} of benzaldehyde) the kinetics were only monitored at or near λ_{max} of BMN (309 nm).

(2) The reaction temperature was 20 °C rather than 25 °C. This is because of the availability of pH calibration scales at 20 °C but not at 25 °C. For better comparison with the results in water we have therefore performed a few experiments in water at 20 °C.

(9) Hallé, J.-C.; Gaboriaud, R.; Schaal, R. *Bull. Soc. Chim. Fr.* **1970**, 2047.

(1) Part 11: Bernasconi, C. F.; Howard, K. A.; Kanavarioti, A. *J. Am. Chem. Soc.* **1984**, *106*, 6827.

(2) Bernasconi, C. F.; Leonarduzzi, G. D. *J. Am. Chem. Soc.* **1982**, *104*, 5133, 5143.

(3) Bernasconi, C. F.; Leonarduzzi, G. D. *J. Am. Chem. Soc.* **1980**, *102*, 1361.

(4) Bernasconi, C. F.; Carré, D. J.; Kanavarioti, A. *J. Am. Chem. Soc.* **1981**, *103*, 4850.

(5) Crowell, T. I.; Kim, T.-R. *J. Am. Chem. Soc.* **1973**, *95*, 6781.

(6) For older work on the hydrolysis of BMN, see: Patai, S.; Rappoport, J. *J. Chem. Soc.* **1962**, 383, 392.

(7) Bernasconi, C. F.; Fox, J. P.; Kanavarioti, A.; Panda, M., in preparation.

(8) Parker, A. *J. Chem. Rev.* **1969**, *69*, 1.

Table I. Initial Slopes, Intercepts, and Plateau Values in the Buffer Catalysis of the Hydrolysis of BMN in 50% Me₂SO–50% Water (v/v) at 20 °C^a

buffer	pH	initial slope, ^b M ⁻¹ s ⁻¹	intercept, ^c s ⁻¹	plateau, ^c s ⁻¹	plateau/intercept
ClCH ₂ CH ₂ COO ⁻	5.17	3.41 × 10 ⁻³	1.32 × 10 ⁻⁴	1.81 × 10 ⁻⁴	1.36 ± 0.08
ClCH ₂ COO ⁻	4.78	4.23 × 10 ⁻⁵	6.88 × 10 ⁻⁵		
CH ₃ COO ⁻	4.72			7.40 × 10 ^{-5 d}	
CH ₃ OCH ₂ COO ⁻	4.70	5.60 × 10 ⁻⁴	5.11 × 10 ⁻⁵	6.81 × 10 ⁻⁵	1.33 ± 0.08
ClCH ₂ COO ⁻	4.55	<i>e</i>	3.68 × 10 ⁻⁵	4.50 × 10 ⁻⁵	1.22 ± 0.07
ClCH ₂ COO ⁻	3.71	5.86 × 10 ⁻⁵	6.41 × 10 ⁻⁶	7.47 × 10 ⁻⁵	1.16 ± 0.07
Cl ₂ CHCOO ⁻	3.40	<i>e</i>	2.20 × 10 ⁻⁶	2.46 × 10 ⁻⁶	1.11 ± 0.06

^a μ = 0.5 M (KCl). ^b Estimated error ±10%. ^c Estimated error ±3%. ^d See text. ^e Uncertain.

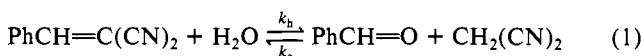
Table II. Initial Slopes, Intercept, and Plateau Values in the Buffer Catalysis of the Hydrolysis of BMN in 60% Me₂SO–40% Water at 20 °C^a

buffer	pH	initial slope, ^b M ⁻¹ s ⁻¹	intercept, ^c s ⁻¹	plateau, ^c s ⁻¹	plateau/intercept
ClCH ₂ CH ₂ COO ⁻	5.60	5.36 × 10 ⁻³	8.68 × 10 ⁻⁶	1.36 × 10 ⁻⁵	1.72
ClCH ₂ COO ⁻	4.70	2.45 × 10 ⁻⁴	3.11 × 10 ⁻⁵	5.44 × 10 ⁻⁵	1.75
ClCH ₂ COO ⁻	4.10	≈ 2.05 × 10 ⁻⁴	1.52 × 10 ⁻⁴	2.61 × 10 ⁻⁴	1.57

^a μ = 0.5 M (KCl). ^b Estimated error ±8%. ^c Estimated error ±3%.

(3) The ionic strength was maintained at 0.5 M with KCl, just as in water, except in 70% Me₂SO–30% water where an ionic strength of 0.25 M was mandated because of the reduced solubility of KCl.

As before¹ we use the following symbols for the rate and equilibrium constants ($K_h = k_h/k_c$) for eq 1.



Rates in 50% Me₂SO–50% Water (v/v). The reaction was studied at pH 5.17 in β-chloropropionate, at pH 4.70 in methoxyacetate, at pH 4.78, 4.55, and 3.71 in chloroacetate, and at pH 3.40 in dichloroacetate buffers. At the three highest pH values the rates were measured in the hydrolysis direction (k_h) while at the other pH values they were measured in the condensation direction. The latter approach was used because of extreme slowness of the hydrolysis in strongly acidic solution.

The condensation experiments were conducted under pseudo-first-order conditions with malononitrile as the excess component. The data were treated according to

$$k_{\text{obsd}} = k_h + k_c[\text{CH}_2(\text{CN})_2]_0 \approx k_c[\text{CH}_2(\text{CN})_2]_0 \quad (2)$$

and k_h was calculated from

$$k_h = k_{\text{obsd}} \frac{K_h}{K_h + [\text{CH}_2(\text{CN})_2]_0} \quad (3)$$

with $K_h = 1.06 \times 10^{-3}$ M obtained from experiments described below.

The results of all buffer experiments are summarized in Tables S1 (pH 5.17, 4.70, 4.78, 32 rate constants) and S2 (pH 4.55, 3.71, 3.40, 15 rate constants) of the supplementary materials.¹⁰ Figure 1 shows two representative plots of k_h vs. buffer base concentration. Both plots are characterized by a steep initial increase in k_h which is followed by a plateau. The plateaus appear to have slightly negative slopes.

Initial slopes, intercepts, and plateau values (obtained by extrapolation of the dashed lines in Figure 1) for all buffers are summarized in Table I. The initial slopes are based on the assumption that it is only the buffer base which is catalytic. The table also includes a "plateau" value for an acetate buffer at pH 4.72 which was obtained at a single (high) acetate ion concentration.

A second series of experiments was performed in HCl solutions (pH 0.29–3.73), again with the rates measured in the condensation direction. In some runs benzaldehyde rather than malononitrile was used as the excess component, with excellent agreement between the two methods. The results are in Table S3¹⁰ (14 rate constants) while Figure 2 shows a pH–rate profile (O). Included

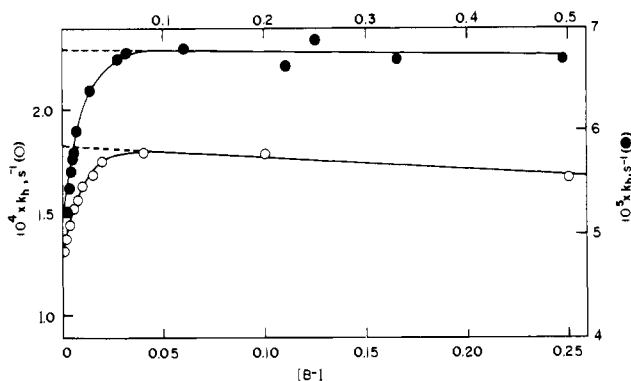


Figure 1. Methoxyacetate catalysis (pH 4.69, ●, right and top axes) and β-chloropropionate catalysis (pH 5.17, ○, left and bottom axes) in 50% Me₂SO–50% water.

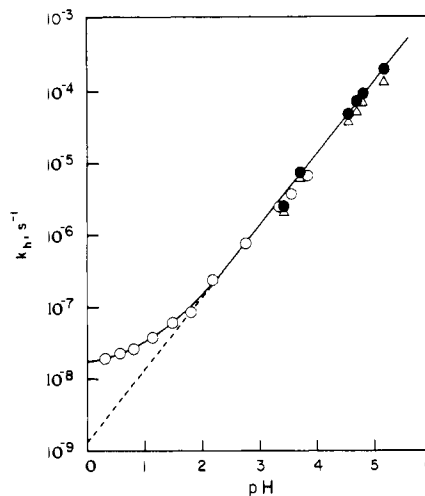


Figure 2. pH–rate profile in 50% Me₂SO–50% water: (O) experiments in HCl solution; (Δ) buffer intercepts (from Table I); (●) buffer plateaus (from Table I).

in the figure are the buffer intercepts (Δ) and plateau values (●) from Table I.

Rates in 60% Me₂SO–40% Water (v/v). In this solvent we studied the dependence on buffer concentration in β-chloropropionate (pH 5.60) and chloroacetate buffers (pH 4.70, 4.10). In the former the rates were measured in the hydrolysis direction, in the latter in the condensation direction. $K_h = 1.00 \times 10^{-3}$ M (see below) was used to calculate k_h according to eq 3.

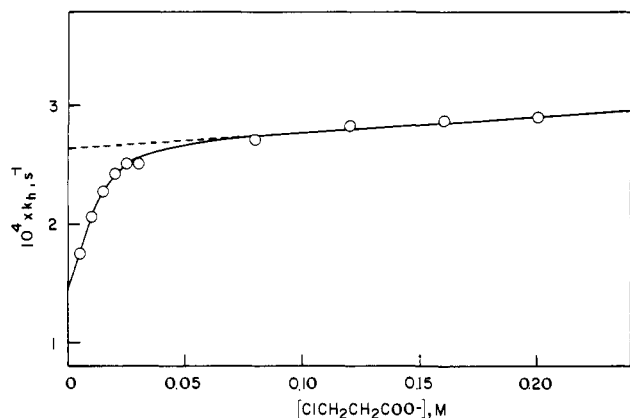
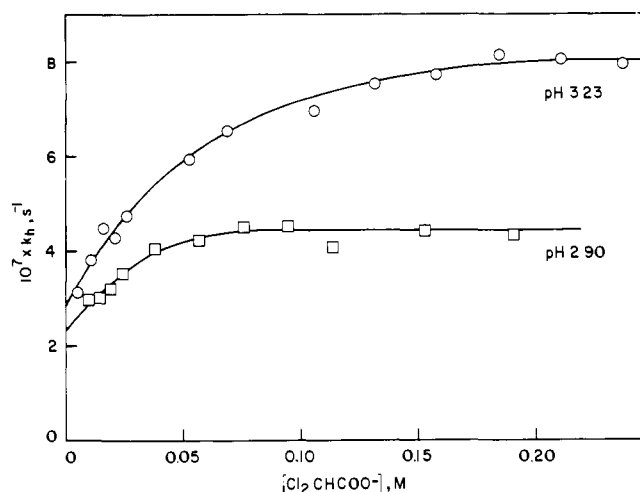
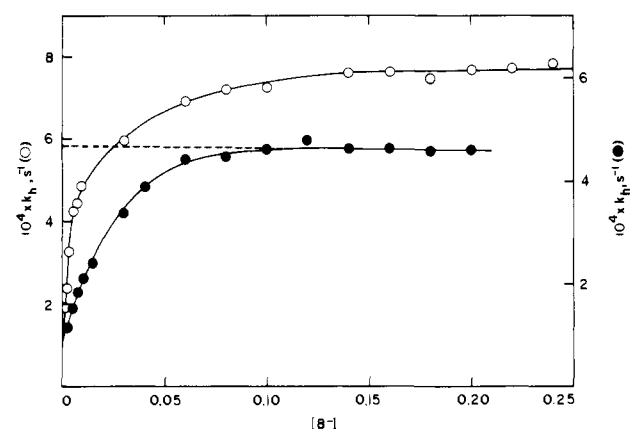
The results are summarized in Table S4¹⁰ (10 rate constants) and S5¹⁰ (16 rate constants), while Figure 3 shows a representative plot of k_h vs. base concentration. The plot shows again a curvilinear dependence as in 50% Me₂SO–50% water, but the extent

(10) See paragraph at the end of this paper regarding supplementary material.

Table III. Initial Slopes, Intercept, and Plateau Values in the Buffer Catalysis of the Hydrolysis of BMN in 70% Me₂SO–30% Water at 20 °C^a

buffer	pH	initial slope, ^b M ⁻¹ s ⁻¹	intercept, ^c s ⁻¹	plateau, ^c s ⁻¹	plateau/intercept
CH ₃ COO ⁻	6.42	4.90 × 10 ⁻²	1.30 × 10 ⁻⁴	7.68 × 10 ⁻⁴	5.91
ClCH ₂ CH ₂ COO ⁻	6.22	1.36 × 10 ⁻²	8.70 × 10 ⁻⁵	4.34 × 10 ⁻⁴	4.99
CH ₃ OCH ₂ COO ⁻	5.72	4.67 × 10 ⁻³	3.25 × 10 ⁻⁵	2.19 × 10 ⁻⁴	6.57
ClCH ₂ COO ⁻	5.00			4.55 × 10 ⁻⁵	
ClCH ₂ COO ⁻	4.90	5.20 × 10 ⁻⁴	6.10 × 10 ⁻⁶		
ClCH ₂ COO ⁻	4.70			2.00 × 10 ⁻⁵	
Cl ₂ CHCOO ⁻	3.23	9.12 × 10 ⁻⁶	2.88 × 10 ⁻⁷	8.00 × 10 ⁻⁷	2.78
Cl ₂ CHCOO ⁻	2.90	4.40 × 10 ⁻⁶	2.35 × 10 ⁻⁷	4.48 × 10 ⁻⁷	1.91

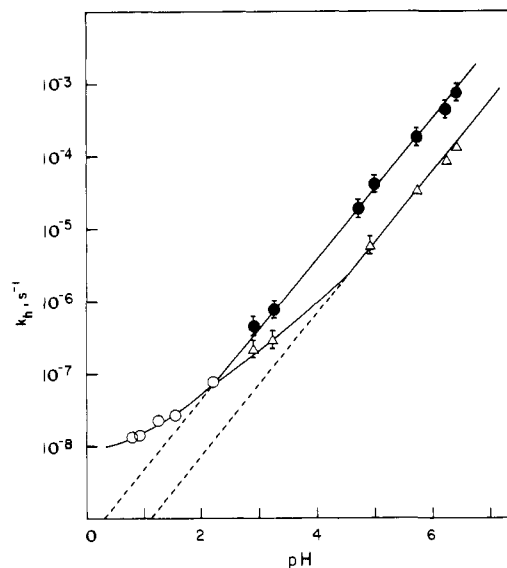
^a μ = 0.25 M (KCl). ^b Estimated error ±5%. ^c Estimated error ±3%.

**Figure 3.** β-Chloropropionate catalysis in 60% Me₂SO–40% water at pH 5.60.**Figure 5.** Dichloroacetate catalysis in 70% Me₂SO–30% water at pH 3.23 and 2.90.**Figure 4.** Acetate catalysis (pH 6.42, O, left axis) and β-chloropropionate catalysis (pH 6.22, ●, right axis) in 70% Me₂SO–30% water.

of the catalysis, as measured by the ratio of plateau/intercept, is significantly larger. The plot also suggests that the plateau is again not strictly horizontal; however, in contrast to the situation in the more aqueous solvent, it is mildly *increasing* with increasing buffer concentration.

Table II summarizes the values for initial slopes, intercepts, and plateaus of the buffer plots.

Rates in 70% Me₂SO–30% Water (v/v). Rates were measured at pH 6.42 in acetate, at pH 6.22 in β-chloropropionate, at pH 5.72 in methoxyacetate, at pH 5.00 in chloroacetate, and at pH 3.23 and 2.90 in dichloroacetate buffers. All buffer data reported here are from experiments conducted in the hydrolysis direction, even in the most acidic buffers where the reaction is very slow. This is because in the strongly acidic chloro- and dichloroacetate buffers the reproducibility of the runs conducted in the condensation direction was not as good as those in the hydrolysis direction. It appears that in 70% Me₂SO there is a reaction between malononitrile and the buffer (or with an impurity in the buffer) which at the high concentrations leads to the slow development of a red color and which interferes with the condensation of malononitrile with benzaldehyde. The nature of this side reaction was not investigated further.

**Figure 6.** pH–rate profile in 70% Me₂SO–30% water: (O) experiments in HCl solution (from Table S8¹⁰); (Δ) buffer intercepts (from Table III); (●) buffer plateaus (from Table III).

Because of the extreme slowness of the hydrolysis below pH 3.5 k_h was determined by the method of initial rates as described in the Experimental Section.

The results of the buffer experiments are summarized in Tables S6¹⁰ (63 rate constants) and S7¹⁰ (24 rate constants) while Figures 4 and 5 show representative buffer plots. The plots are again curvilinear, but the extent of the catalysis is much greater than in the other two solvents. This is reflected in plateau/intercept ratios in the order of 5–6 in the more basic buffers (Table III); in the two most acidic buffers this ratio is significantly reduced.

As in 50% Me₂SO–50% water some determinations were also made in HCl solutions. Since no problems were encountered in measuring the rates in the condensation direction, this was the

method of choice for these extremely slow reactions. The results are in Table S8¹⁰ (5 rate constants) while Figure 6 shows a logarithmic plot of k_h vs. pH (O); the figure also includes the intercepts (Δ) and plateau values (\bullet) of the buffer plots taken from Table III.

A few experiments were conducted aimed at examining the potential role played by specific salt effects. To this end KCl was replaced by potassium chloroacetate as the compensating electrolyte in some runs conducted in β -chloropropionate buffer. In one series of experiments pairs of runs at a given buffer concentration were compared where in one of the runs the compensating electrolyte was KCl, in the other KOOCCH₂Cl. The results are summarized in Table S9¹⁰ (part A). k_h was observed to be between 2% and 6% higher with KOOCCH₂Cl as the compensating electrolyte. This increase is barely outside the experimental error and is considered insignificant. This conclusion is supported by the results of a second series of experiments (Table S9, part B) in which the effect of gradually replacing KCl with KOOCCH₂Cl at constant buffer concentration was investigated. Slight variations ($\pm 3\%$) were observed, but they were essentially random.

Rates in Water at 20 °C. The rate of hydrolysis of BMN was measured at five different pH values from pH 3.11 to 3.96 in methoxyacetate buffers at a single buffer concentration.¹¹ The results are in Table S10.¹⁰ A plot (not shown) of k_h vs. $a_{H^+}^{-1}$ is linear with a slope = $2.15 \times 10^{-9} \text{ M}^{-1} \text{ s}^{-1}$.

Equilibrium Constants at 50%, 60%, and 70% Me₂SO and in Water. The equilibrium constant, K_h , of reaction 1 was determined kinetically. The rates were measured in the condensation direction, usually with malononitrile as the excess component but in some cases with benzaldehyde in excess. k_{obsd} was measured at various concentrations of the excess component and is given by

$$k_{\text{obsd}} = k_h + k_c[\text{E.C.}]_0 \quad (4)$$

with [E.C.]₀ being the concentration of the excess component.

The range of concentrations was chosen as to provide good values for both k_h (intercept) and k_c (slope). The results are summarized in Tables S11–S14.¹⁰ The following K_h values were obtained: 1.06×10^{-3} M in 50% Me₂SO, 1.00×10^{-3} M in 60% Me₂SO, 8.21×10^{-4} M in 70% Me₂SO, and 3.22×10^{-3} M in water.

Discussion

Mechanism of Buffer Catalysis. In all three Me₂SO-containing solvents there is a curvilinear dependence of k_h on buffer concentration (Figures 1 and 3–5). We attribute this buffer dependence to general base catalysis as detailed below. In 50% Me₂SO the catalytic effect is quite small, though, with a total increase in k_h ranging from $\sim 11\%$ at the lowest pH to $\sim 36\%$ at the highest pH (plateau/intercept ratios in Table I). Such small increases raise the question whether we might be witnessing a specific salt or medium effect rather than authentic base catalysis; some reactions measured in mixed solvents are known to be particularly prone to such effects.^{12,13}

In view of the fact that the catalytic effects occur at very low base concentration (0.01 to 0.02 M) this seems an unattractive interpretation.^{13b} On the other hand, specific salt effects, or medium effects caused by the buffer acid, may play a role at high buffer concentration. The slightly sloping plateaus in 50% and 60% Me₂SO (Figures 1 and 3) are probably caused by such effects although it is not clear why the sign of the slopes changes from 50% to 60% Me₂SO and why no such effects are observed in 70% Me₂SO. Irrespective of the detailed interpretation of the sloping plateau, the effects are very small and barely outside the error limits, as is also confirmed by our limited investigation of salt effects (Table S9¹⁰).

The curvilinear dependence of k_h on base concentration indicates a change in rate-controlling step. In any given solvent the change

always occurs at about the same buffer acid concentration. This behavior is easily understood in terms of a change from rate-limiting (or co-limiting) oxygen deprotonation of T^o_{OH} at low buffer concentration to rate-limiting breakdown of T^o_O at high concentration, as previously observed in the hydrolysis of *p*-nitrobenzylidene Meldrum's acid.²

The expression for k_h , derived by means of the steady-state approximation for T^o_O and by assuming that the first two steps in Scheme I are rapid equilibria,¹ is given by

$$k_h = \frac{K_1 \text{H}_2\text{O}}{K_a^{\text{CH}}} \left\{ \frac{(k_3 \text{H}_2\text{O} + k_3^{\text{B}}[\text{B}] + k_3^{\text{OH}} a_{\text{OH}^-}) k_4}{k_{-3}^{\text{H}} a_{\text{H}^+} + k_{-3}^{\text{BH}} [\text{BH}] + k_{-3}^{\text{H}_2\text{O}} + k_4} + k_{34} \text{H}_2\text{O} \right\} \quad (5)$$

$K_1 \text{H}_2\text{O}$ is the equilibrium constant for water addition to BMN (to form T^o_{OH} + H⁺) while K_a^{CH} is the C–H acid dissociation constant of T^o_{OH}. Note that eq 5 contains a $k_{34} \text{H}_2\text{O}$ term for the direct conversion of T^o_{OH} to malononitrile and benzaldehyde which becomes dominant in strongly acidic solution, as discussed below.

According to eq 5 the initial slopes of the buffer plots are given by

$$\text{slope} = \frac{K_1 \text{H}_2\text{O}}{K_a^{\text{CH}}} \frac{k_3^{\text{B}} k_4}{k_{-3}^{\text{H}} a_{\text{H}^+} + k_{-3}^{\text{H}_2\text{O}} + k_4} \quad (6)$$

Equation 5 also shows that it is indeed the buffer acid concentration (and/or a_{H^+}) which determines the change in rate-limiting step: at high [BH] ($k_{-3}^{\text{BH}} [\text{BH}] \gg k_4$) and/or high a_{H^+} ($k_{-3}^{\text{H}} a_{\text{H}^+} \gg k_4$) eq 1 simplifies to

$$k_h = \frac{K_1 \text{H}_2\text{O}}{K_a^{\text{CH}}} \left\{ \frac{K_a^{\text{OH}}}{a_{\text{H}^+}} k_4 + k_{34} \text{H}_2\text{O} \right\} \quad (7)$$

with K_a^{OH} being the O–H acid dissociation constant of T^o_{OH}.

It is the k_h values determined in HCl solution (O in Figures 2 and 6) and the plateau values of the buffer plots (\bullet in Figures 2 and 6) which obey eq 7. The pH–rate profiles in Figures 2 and 6 show that the pH-independent $k_{34} \text{H}_2\text{O}$ term starts to become important below pH 2.

At zero buffer concentration eq 5 becomes

$$k_h = \frac{K_1 \text{H}_2\text{O}}{K_a^{\text{CH}}} \left\{ \frac{(k_3 \text{H}_2\text{O} + k_3^{\text{OH}} a_{\text{OH}^-}) k_4}{k_{-3}^{\text{H}} a_{\text{H}^+} + k_{-3}^{\text{H}_2\text{O}} + k_4} + k_{34} \text{H}_2\text{O} \right\} \quad (8)$$

This corresponds to the intercepts of the buffer plots (Δ in Figures 2 and 6). At pH values such that $k_{-3}^{\text{H}} a_{\text{H}^+} \ll k_{-3}^{\text{H}_2\text{O}}$ and $k_3^{\text{H}_2\text{O}} \ll k_3^{\text{OH}} a_{\text{OH}^-}$ eq 8 further simplifies to¹⁴

$$k_h = \frac{K_1 \text{H}_2\text{O}}{K_a^{\text{CH}}} \frac{k_4 k_3^{\text{OH}} a_{\text{OH}^-}}{k_{-3}^{\text{H}_2\text{O}} + k_4} \quad (9)$$

Hence, in the pH range where eq 9 is valid the pH–rate profiles for plateaus (eq 7) and intercepts (eq 9) should be parallel as is clearly visible in Figure 6 at pH ~ 4.5 to 6.5. At lower pH where the $k_3^{\text{H}_2\text{O}}$ and $k_{-3}^{\text{H}} a_{\text{H}^+}$ terms (eq 8) are no longer negligible the two lines are no longer parallel.

These observations are best treated quantitatively by focusing on the ratios of plateau/intercept. These ratios are summarized in Tables I–III. At pH > 2 where the $k_{34} \text{H}_2\text{O}$ term can be neglected both in eq 7 and 8 we have

$$\begin{aligned} \frac{\text{plateau}}{\text{intercept}} &= \frac{K_a^{\text{OH}} k_{-3}^{\text{H}_2\text{O}} + k_{-3}^{\text{H}} a_{\text{H}^+} + k_4}{a_{\text{H}^+} k_3^{\text{OH}} a_{\text{OH}^-} + k_3^{\text{H}_2\text{O}}} \\ &= \frac{k_{-3}^{\text{H}_2\text{O}} + k_{-3}^{\text{H}} a_{\text{H}^+} + k_4}{k_{-3}^{\text{H}_2\text{O}} + k_{-3}^{\text{H}} a_{\text{H}^+}} = 1 + \frac{k_4}{k_{-3}^{\text{H}_2\text{O}} + k_{-3}^{\text{H}} a_{\text{H}^+}} \end{aligned} \quad (10)$$

After rearranging and inverting eq 10 one obtains

$$\left\{ \frac{\text{plateau}}{\text{intercept}} - 1 \right\}^{-1} = \frac{k_{-3}^{\text{H}_2\text{O}}}{k_4} + \frac{k_{-3}^{\text{H}} a_{\text{H}^+}}{k_4} \quad (11)$$

(14) At these pH values the $k_{34} \text{H}_2\text{O}$ term is negligible.

(11) No buffer dependence is expected since there is none at 25 °C.¹

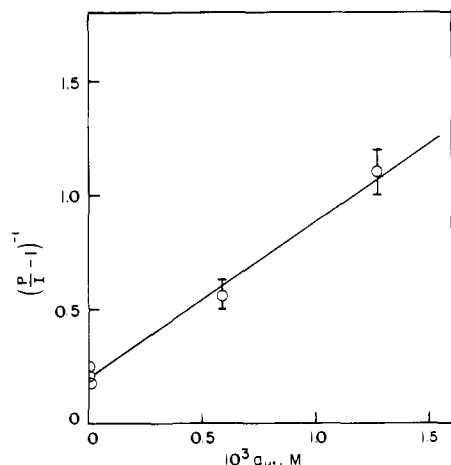
(12) (a) Bockris, J. O'M.; Egan, H. *Trans. Faraday Soc.* **1948**, *44*, 151. (b) Grunwald, E.; Butler, A. F. *J. Am. Chem. Soc.* **1960**, *82*, 5647.

(13) (a) Salomaa, P.; Kankaanperä, A.; Lahti, M. *J. Am. Chem. Soc.* **1971**, *93*, 2084. (b) Hand, E. S.; Jencks, W. P. *J. Am. Chem. Soc.* **1975**, *97*, 6221.

Table IV. Summary of Rate and Equilibrium Constants at 20 °C^a

no.	parameter	water	50% Me ₂ SO	60% Me ₂ SO	70% Me ₂ SO
1	$k_{-3}^H/k_4, M^{-1}$		$\sim 1.7 \times 10^4$	$\sim 4.8 \times 10^3$	$6.8 \pm 1.5 \times 10^2$
2	$k_{-3}^{H_2O}/k_4$		3.0 ± 0.4	1.3 ± 0.1	0.21 ± 0.03
3	$k_{-3}^H, M^{-1} s^{-1}$	$\sim 4.0 \times 10^{10}$	$\sim 1.0 \times 10^{10}$	$\sim 0.75 \times 10^{10}$	$\sim 0.40 \times 10^{10}$
4	k_4, s^{-1}	$\sim 3.3 \times 10^4$	$\sim 5.9 \times 10^5$	$\sim 1.6 \times 10^6$	$\sim 5.9 \times 10^6$
5	$k_{-4}, M^{-1} s^{-1}$	$\sim 1.5 \times 10^5$	$\sim 1.4 \times 10^4$	$\sim 7.9 \times 10^3$	$\sim 3.0 \times 10^3$
6	K_4, M	$\sim 2.1 \times 10^{-1}$	$\sim 4.3 \times 10^1$	$\sim 2.0 \times 10^2$	$\sim 2.0 \times 10^3$
7	$k_{-3}^{H_2O}, s^{-1}$		$\sim 2.0 \times 10^6$	$\sim 2.0 \times 10^6$	$\sim 1.2 \times 10^6$
8	$k_3^{OH}, M^{-1} s^{-1}$		$\sim 1.5 \times 10^9$	$\sim 1.5 \times 10^9$	$\sim 1.5 \times 10^9$
9	pK_w	14.00	15.90	16.67	17.79
10	pK_a^{OH}	~ 11.2	~ 13.0	~ 13.8	~ 14.7
11	$K_1^{H_2O}/K_a^{CH}$	$\sim 1.0 \times 10^{-2}$	$\sim 1.5 \times 10^{-2}$	$\sim 2.8 \times 10^{-2}$	$\sim 2.5 \times 10^{-2}$
12	K_h, M	3.22×10^{-2}	1.06×10^{-3}	1.00×10^{-3}	8.21×10^{-4}
13	$pK_a^{CH_2(CN)_2}$	11.39	10.21	10.05	9.92
14	$(K_1^{H_2O}/K_a^{CH})k_{34}^{H_2O}$		1.60×10^{-8}		1.20×10^{-8}
15	$k_{34}^{H_2O}, s^{-1}$	$\sim 1.0 \times 10^{-6}$	1.05×10^{-6}		4.76×10^{-7}
16	$k_{34}^{H_2O}/[H_2O], M^{-1} s^{-1}$	$\sim 1.8 \times 10^{-8}$	3.78×10^{-8}		2.85×10^{-8}
17	$K_{34}^{H_2O}$	~ 0.33	$\sim 6.9 \times 10^{-2}$		$\sim 3.25 \times 10^{-2}$

^a $\mu = 0.5$ M except in 70% Me₂SO where $\mu = 0.25$ M.

Figure 7. Plot according to eq 11 in 70% Me₂SO–30% water.

A plot according to eq 11 is shown in Figure 7 for 70% Me₂SO. It affords $k_{-3}^{H_2O}/k_4 = 0.21 \pm 0.03$ and $k_{-3}^H/k_4 = 6.8 \pm 1.5 \times 10^2 M^{-1}$. A similar analysis of the data in the other solvents leads to $k_{-3}^{H_2O}/k_4 = 3.0 \pm 0.3$ in 50% Me₂SO and 1.3 ± 0.1 in 60% Me₂SO while for k_{-3}^H/k_4 only crude estimates can be obtained ($\sim 1.7 \times 10^4 M^{-1}$ in 50%, $\sim 4.8 \times 10^3 M^{-1}$ in 60% Me₂SO).

Dissection of Individual Rate and Equilibrium Constants. Table IV provides a summary of various rate and equilibrium constants in water and in 50%, 60%, and 70% aqueous Me₂SO, all at 20 °C. This section details how they were obtained on the basis of our results, coupled with a few assumptions about diffusion or nearly diffusion-controlled proton transfers.

$k_{-3}^H, k_{-3}^{H_2O}$, and k_4 . Our estimates for k_{-3}^H in the four solvents are listed under no. 3 in Table IV. They are based on rate constants of $3\text{--}5 \times 10^{10} M^{-1} s^{-1}$ for the diffusion-controlled protonation of strongly basic oxyanions by H₃O⁺ in water¹⁵ and the following two corrections in the Me₂SO containing solvents. (1) The $\sim 3.5\text{--}4.4$ -fold higher viscosity of our Me₂SO–water mixtures¹⁶ should reduce k_{-3}^H by corresponding factors.¹⁹ If we take a value of $4 \times 10^{10} M^{-1} s^{-1}$ in water, k_{-3}^H in 50%, 60%, and 70% Me₂SO would be 1.16×10^{10} , 0.95×10^{10} , and $0.91 \times 10^{10} M^{-1} s^{-1}$, respectively.¹⁶

(2) An additional small downward adjustment has been applied because the smaller water concentration in the mixed solvents²⁰ is expected to reduce the effectiveness of the proton-jump mechanism.^{15,19} In estimating the amount of this additional reduction we were guided by its effect on the value of pK_a^{OH} calculated from it, as discussed below.

A third factor which might reduce k_{-3}^H in all solvents about equally is the possibility of steric hindrance in the approach to the relatively bulky T⁻. However, because of the small size of H₃O⁺ and the availability of the proton-jump mechanism^{15,19} such steric effects generally become significant only when the base is extremely crowded.²¹ This is hardly the case for T⁻ and thus a significant steric retardation seems unlikely.

Coupled with the experimental k_{-3}^H/k_4 ratios (no. 1), our estimates for k_{-3}^H allow us now to estimate k_4 (no. 4) and from the experimental $k_{-3}^{H_2O}/k_4$ ratios (no. 2) we also obtain $k_{-3}^{H_2O}$ (no. 7) in the mixed solvents. It should be noted that k_4 and $k_{-3}^{H_2O}$ obtained in this manner are probably fairly reliable in 70% Me₂SO but less so in 50% and 60% Me₂SO because of the large uncertainty in k_{-3}^H/k_4 . However, independent estimates discussed below show that our values in 50% and 60% Me₂SO are quite reasonable.

In water k_4 was obtained from k_h measured between pH 3.11 and 3.96 (Table S10);¹⁰ in this range k_h obeys eq 7,¹ and $K_1^{H_2O}/K_a^{CH}$ and K_a^{OH} were estimated as discussed below.

k_3^{OH} and pK_a^{OH} . For k_3^{OH} we have assumed a value of $1.5 \times 10^9 M^{-1} s^{-1}$ in all solvents (no. 8). This value is an average based on direct experimental determination of k_3^{OH} in various similar systems, both in water and in 50% Me₂SO.²³ Together with $k_{-3}^{H_2O}$ and the ionic product of the solvent (no. 9) we now obtain pK_a^{OH} in the Me₂SO–water mixtures (no. 10).

A different method for estimating pK_a^{OH} is based on a Taft correlation²⁴ which leads to $pK_a^{OH} = 11.1$ in water at 25 °C.¹ Since pK_w is slightly higher at 20 °C than at 25 °C,²⁵ pK_a^{OH} is likely to be slightly higher, too. We shall assume $pK_a^{OH} = 11.2$ in water at 20 °C. Upon addition of Me₂SO the pK_a of an alcohol is expected to increase nearly as much as pK_w .⁹ The pK_a^{OH} values listed in Table IV which were estimated on the basis of k_3^{OH} and $k_{-3}^{H_2O}$ are seen to reflect this expectation quite well: For the change from water to 50% Me₂SO we have $\Delta pK_a^{OH} = 1.8$, $\Delta pK_w = 1.90$; for the change from 50% to 60% Me₂SO $\Delta pK_a^{OH} = 0.8$, $\Delta pK_w = 0.77$; for the change from 60% to 70% Me₂SO $\Delta pK_a^{OH} = 0.9$, $\Delta pK_w = 1.13$. This consistency indicates that our estimates of pK_a^{OH} cannot be far off the mark.

(15) (a) Eigen, M. *Angew. Chem., Int. Ed. Engl.* **1964**, *3*, 1. (b) Eigen, M.; Kruse, W.; Maass, G.; DeMaeyer, L. *Prog. React. Kinet.* **1964**, *2*, 287.

(16) The viscosities in water and 50%, 60%, and 70% Me₂SO are 1.002,¹⁷ 3.455,¹⁸ ~ 4.2 ,¹⁸ and ~ 4.4 ¹⁸ cP, respectively.

(17) Weast, R. C., Ed. "Handbook of Chemistry and Physics", The Chemical Rubber Co.: Cleveland, Ohio, 1971; p F-36.

(18) Janz, G. J.; Tompkins, R. P. T. "Nonaqueous Electrolyte Handbook," Academic Press: New York, 1972; Vol. 1, p 1043.

(19) Crooks, J. E. *Compr. Chem. Kinet.* **1977**, *8*, 197.

(20) [H₂O] = 55.5, 27.8, 22.2, and 16.7 M, respectively.

(21) Bernasconi, C. F.; Carré, D. J. *J. Am. Chem. Soc.* **1979**, *101*, 2698, 2707.

(22) Weller, A. *Prog. React. Kinet.* **1961**, *1*, 189.

(23) For example, in the hydrolysis of *p*-nitrobenzylidene Meldrum's acid $k_3^{OH} = 1.8 \times 10^9 M^{-1} s^{-1}$ in water,^{3a} and in the hydrolysis of 1,1-dinitro-2,2-diphenylethylene $k_3^{OH} = 1.3 \times 10^9 M^{-1} s^{-1}$ in 50% Me₂SO–50% water.⁴

(24) Takahashi, S.; Cohen, L. A.; Miller, H. K.; Peake, E. G. *J. Org. Chem.* **1971**, *36*, 1205.

(25) Reference 17, p D-122.

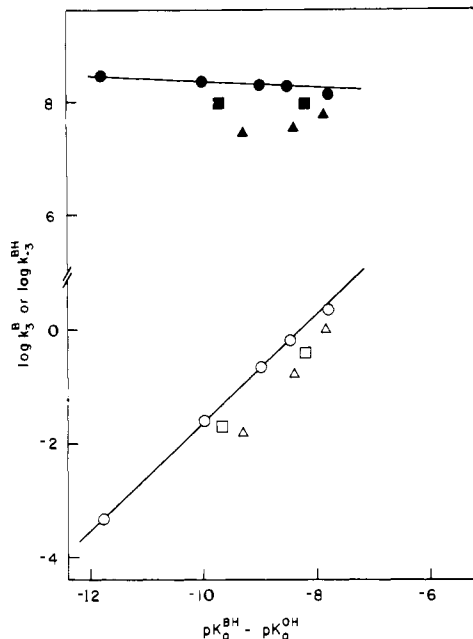


Figure 8. Eigen plot for the proton transfer $T^{\circ}OH + B^- \rightleftharpoons T^{\circ}O + BH$. Open symbols, k_3^B ; filled symbols, k_3^{BH} . Circles, 70% Me₂SO; squares, 60% Me₂SO; triangles, 50% Me₂SO.

$K_1^{H_2O}/K_a^{CH}$, K_4 , $k_{34}^{H_2O}$, and $K_{34}^{H_2O}$. The $K_1^{H_2O}/K_a^{CH}$ ratios (no. 11) in the Me₂SO–water mixtures can be obtained from

$$\frac{K_1^{H_2O}}{K_a^{CH}} = \frac{\text{intercept}}{k_3^{OH} a_{OH^-}} \left(\frac{k_3^{H_2O}}{k_4} + 1 \right) \quad (12)$$

which is derived from eq 9. It should be noted that eq 12 contains the more reliable $k_3^{H_2O}/k_4$ ratio rather than the less certain k_3^H/k_4 ratio and hence our $K_1^{H_2O}/K_a^{CH}$ values are as good as our estimate for k_3^{OH} which is considered quite reliable.

In water we have assumed that $K_1^{H_2O}/K_a^{CH}$ is $2/3$ of its value in 50% Me₂SO, based on the slight increase in this ratio observed when the medium becomes richer in Me₂SO.

We now obtain the equilibrium constants for the breakdown of $T^{\circ}O$ into benzaldehyde and $CH(CN)_2^-$ (K_4 , no. 6), and for the breakdown of $T^{\circ}OH$ into benzaldehyde and $CH_2(CN)_2$ ($K_{34}^{H_2O}$, no. 17), via

$$K_4 = K_h \frac{K_a^{CH} K_a^{CH_2(CN)_2}}{K_1^{H_2O} K_a^{OH}} \quad (13)$$

$$K_{34}^{H_2O} = K_a^{OH} K_4 / K_a^{CH_2(CN)_2} \quad (14)$$

Finally, from the plateaus of the pH–rate profiles in 50% (Figure 2) and 70% Me₂SO (Figure 6) $k_{34}^{H_2O}$ (no. 15) is found via eq 7. In water $k_{34}^{H_2O}$ was estimated on the basis of the value found at 25 °C and assuming the same temperature dependence as for k_4 .

k_3^B and k_3^{BH} . With $K_1^{H_2O}/K_a^{CH}$ being known we now evaluate the rate constants for oxygen deprotonation of $T^{\circ}OH$ by buffer bases from the initial slopes of the buffer plots. Rearranging eq 6 provides

$$k_3^B = \text{slope} \frac{K_a^{CH}}{K_1^{H_2O}} \left(\frac{k_3^{H_2O}}{k_4} + \frac{k_3^H a_{H^+}}{k_4} + 1 \right) \quad (15)$$

k_3^{BH} is obtained as $k_3^B K_a^{BH}/K_a^{OH}$ with K_a^{BH} being the acid dissociation constant of the buffer. The k_3^B and k_3^{BH} values are summarized in Table V.

Rates of Proton Transfer. Figure 8 shows Eigen plots^{15a} for the reaction

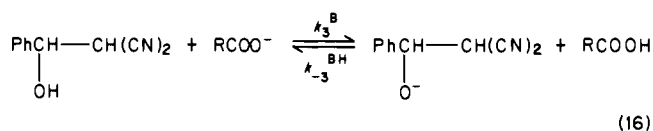


Table V. Rate Constants for the Proton Transfer, $T^{\circ}OH \rightleftharpoons T^{\circ}O^a$

	50% Me ₂ SO ($pK_a^{OH} \sim 13.0$)	60% Me ₂ SO ($pK_a^{OH} \sim 13.8$)	70% Me ₂ SO ($pK_a^{OH} \sim 14.7$)
AcO ⁻ /AcOH			
k_3^B			2.3
k_3^{BH}			1.4×10^8
pK_a^{BH}			6.90
$pK_a^{BH} - pK_a^{OH}$			-7.8
ClCH ₂ CH ₂ COO ⁻ /ClCH ₂ CH ₂ COOH			
k_3^B	9.1×10^{-1}	4.4×10^{-1}	6.5×10^{-1}
k_3^{BH}	6.2×10^7	7.4×10^7	1.9×10^8
pK_a^{BH}	5.17	5.60	6.22
$pK_a^{BH} - pK_a^{OH}$	-7.83	-8.20	-8.48
MeOCH ₂ COO ⁻ /MeOCH ₂ COOH			
k_3^B	1.6×10^{-1}		2.2×10^{-1}
k_3^{BH}	3.9×10^7		2.0×10^8
pK_a^{BH}	4.60		5.72
$pK_a^{BH} - pK_a^{OH}$	-8.40		-8.98
ClCH ₂ COO ⁻ /ClCH ₂ COOH			
k_3^B	1.9×10^{-2}	1.9×10^{-2}	2.5×10^{-2}
k_3^{BH}	3.7×10^7	9.8×10^7	2.4×10^8
pK_a^{BH}	3.71	4.10	4.70
$pK_a^{BH} - pK_a^{OH}$	-9.29	-9.70	-10.00
Cl ₂ CHCOO ⁻ /Cl ₂ CHCOOH			
k_3^B			4.7×10^{-4}
k_3^{BH}			2.7×10^8
pK_a^{BH}			2.92
$pK_a^{BH} - pK_a^{OH}$			-11.78

^a In units of M⁻¹ s⁻¹.

It should be noted that even though the absolute values of k_3^B and k_3^{BH} depend on our estimates of $K_1^{H_2O}/K_a^{CH}$ and pK_a^{OH} , their relative values in a given solvent which determine the shape of the Eigen plots do not depend on these estimates.

In 70% Me₂SO buffer catalysis is quite strong and thus the initial slopes from which k_3^B is calculated are undoubtedly the most accurate. This is also the solvent in which the largest number of buffers was studied. The five points in this solvent (○ and ● in Figure 8) define two excellent straight lines whose slopes are $\beta = 0.96 \pm 0.05$ (k_3^B) and $\alpha = 0.05 \pm 0.05$ (k_3^{BH}). These slopes which are indistinguishable from 1.0 and 0.0, respectively, are typical for diffusion-controlled proton transfers.¹⁵

The results in 50% and 60% Me₂SO, even though more scattered, obey the same pattern as in 70% Me₂SO. A $\beta = 1.0$ was also found for the k_3^B step in the hydrolysis of *p*-nitrobenzylidene Meldrum's acid in water.²

It is noteworthy that the values for k_3^{BH} are all significantly below the diffusion-controlled limit. On the basis of the work by Eigen¹⁵ and his school²⁶ one expects the diffusion-controlled limit to be $\sim 10^{10}$ M⁻¹ s⁻¹ in water and between ~ 2.3 and 2.9×10^9 M⁻¹ s⁻¹ in the more viscous Me₂SO–water mixtures.^{16,19} Our values vary between 3.7×10^7 (ClCH₂COOH in 50% Me₂SO) and 2.7×10^8 M⁻¹ s⁻¹ (ClCH₂CH₂COOH in 70% Me₂SO), i.e., they are from ~ 10 - to ~ 70 -fold lower than expected. This indicates the presence of a steric effect. Such steric effects on proton transfers between normal acids and bases which still show the typical limiting $\beta = 1.0$ and $\alpha = 0.0$ Brønsted coefficients for diffusion-controlled proton transfer are not uncommon.^{21,22,27–29}

Molecular models suggest, though, that the steric crowding in the encounter complex is only moderate and does not prevent the reactants from coming into close proximity, particularly if one allows for the proton transfer to proceed through a water bridge.¹⁵ The steric retardation can, however, be understood in terms of Weller's²² model in which the rate constant may be expressed as

$$k_3^{BH} = k_D \sigma_{BH} \sigma_{T^{\circ}O} \quad (17)$$

(26) Ahrens, M.-L.; Maass, G. *Angew. Chem., Int. Ed. Engl.* **1968**, *7*, 818.

(27) (a) Bernasconi, C. F. *Acc. Chem. Res.* **1978**, *11*, 147. (b) Bernasconi, C. F.; Muller, M. C.; Schmid, P. *J. Org. Chem.* **1979**, *44*, 3189.

(28) Bernasconi, C. F.; Murray, C. J.; Fox, J. P.; Carré, D. *J. Am. Chem. Soc.* **1983**, *105*, 4349.

(29) Barnett, G. H.; Hibbert, F. *J. Am. Chem. Soc.* **1984**, *106*, 2080.

Table VI. Solvent Activity Coefficients for the Transfer from Water to Me₂SO–Water Mixtures

	50% Me ₂ SO	60% Me ₂ SO	70% Me ₂ SO
$\log \gamma_{T-O}^D$ ^a	≈3.25	≈4.25	≈5.54
$\log \gamma_{PhCHO}^D$ ^b	≈0	≈0	≈0
$\log \gamma_{CH(CN)_2}^D$ ^c	≈0.75	≈0.93	≈1.13
$\log \gamma_{CH_2(CN)_2}^D$ ^b	≈0	≈0	≈0
$\log \gamma_{H^+}^D$ ^d	-1.93	-2.27	≈-2.60
$\delta \log K_4^D$ (eq 18)	≈2.50	≈3.32	≈4.41
$\delta \log K_4^D$ (obsd)	2.31	2.98	3.98

^a Assumed to be equal to $\log \gamma_{OH^-}^D$, from ref 30. ^b Assumed values. ^c Calculated via eq 19, see text. ^d From ref 30.

k_D is the diffusional rate constant given by the Smoluchowski equation¹⁹ while σ_{BH} and σ_{T-O} are the steric factors of the two reactants. These steric factors can be visualized as the spatial angles into which the proton can be donated (σ_{T-O}), or from which it can be removed (σ_{BH}), respectively. The molecular models suggest that σ_{T-O} is indeed quite small which makes the relatively small values of k_{-3}^{BH} plausible.

Whether our finding that the k_{-3}^{BH} values in 70% Me₂SO are somewhat higher than in the other two solvents represents a real phenomenon (it is unlikely that the lower ionic strength in 70% Me₂SO is responsible for the higher rates) or whether it is an artifact caused by an accumulation of errors mainly in the more aqueous solvents is difficult to tell. The low k_{-3}^{BH} for ClCH₂C(OOH) and MeOCH₂COOH in 50% Me₂SO is almost certainly the result of our difficulty in measuring accurate slopes for the very weak catalysis. If these two values are ignored the discrepancies between the k_{-3}^{BH} values in the different solvents are less than a factor of 3.

Our present findings suggest that our earlier estimate of $k_{-3}^{BH} \approx 10^{10} \text{ M}^{-1} \text{ s}^{-1}$ for the protonation of T_O derived from benzylidene Meldrum's acid^{3a} by carboxylic acids in water needs to be revised downward. A value of $\sim 2 \times 10^8 \text{ M}^{-1} \text{ s}^{-1}$, reflecting the fact that T_O derived from Meldrum's acid is sterically somewhat bulkier than T_O derived from BMN (smaller σ_{T-O} in eq 17), seems reasonable. This new estimate requires a corresponding adjustment in the pK_a^{OH} from 14.45³ to 12.8 for benzylidene Meldrum's acid.

Solvent Effects on k_4 and K_4 . Both k_4 and K_4 increase quite strongly with added dimethyl sulfoxide. The total increase from water to 70% Me₂SO amounts to a factor of ≈ 180 for k_4 (no. 4 in Table IV) and of nearly 10^4 for K_4 (no. 6). These increases are best understood in terms of a destabilization of the anionic oxygen in T_O which leads to an increased push on the departing CH(CN)₂⁻. This destabilization is partly but not entirely (see below) reflected in the higher pK_a^{OH} values in the Me₂SO-containing solvents (no. 10).

Even though the decreased solvation of the anionic oxygen is the main factor which determines the solvent effect on the breakdown of T_O, changes in the solvation of the products are also expected to affect this solvent effect. Equation 18 expresses the solvent dependence of K_4 in terms of solvent activity coefficients⁸ for the transfer from water to the Me₂SO-containing solvent of each species involved in the equilibrium.

$$\delta \log K_4^D = \log \gamma_{T-O}^D - \log \gamma_{PhCHO}^D - \log \gamma_{CH(CN)_2}^D \quad (18)$$

The solvent activity coefficients of these species are not known but can be estimated as follows. For T_O we assume that γ_{T-O}^D is approximately the same as for OH⁻ ($\gamma_{OH^-}^D$ is known³⁰) while $\log \gamma_{PhCHO}^D$ is assumed to be ≈ 0 as is, e.g., the case for acetylacetone.³¹ $\log \gamma_{CH(CN)_2}^D$ is estimated from

$$\Delta p^{WK^D}_{CH_2(CN)_2} = \log \gamma_{CH(CN)_2}^D + \log \gamma_{H^+}^D - \log \gamma_{CH_2(CN)_2}^D \quad (19)$$

with $\Delta p^{WK^D}_{CH_2(CN)_2}$ being the solvent effect on the pK_a of malononitrile (no. 13 in Table IV), $\log \gamma_{H^+}^D$ being known,³⁰ and

(30) Wells, C. F. In "Thermodynamic Behavior of Electrolytes in Mixed Solvents-II;" Furter, W. F., Ed.; *Adv. Chem. Ser.* 1979, 177, 53.

$\log \gamma_{CH_2(CN)_2}^D$ assumed to be ≈ 0 .

Our estimates are summarized in Table VI; the table also includes the experimental $\delta \log K_4^D$ values as well as $\delta \log K_4^D$ calculated according to eq 18. The agreement between the calculated and observed $\delta \log K_4^D$ values is quite good and indicates that our approach is basically sound.³²

The most interesting conclusion to be drawn is that the increase in K_4 in the Me₂SO-containing solvents is entirely due to the destabilization of T_O, and that its effect on K_4 would be even larger if it were not attenuated by the destabilization of CH(CN)₂⁻ ($\log \gamma_{CH(CN)_2}^D > 0$).³³

Since $\delta \log K_4^D$ obeys eq 18 (with $\log \gamma_{PhCHO}^D \approx 0$) quite well one may expect that the solvent effect on k_4 may be expressed by an equation of the form

$$\delta \log k_4^D = \beta_{N,sol} \log \gamma_{T-O}^D - \beta_{I,sol} \log \gamma_{CH(CN)_2}^D \quad (20)$$

The equation bears a formal resemblance to

$$\delta \log k = \beta \delta(pK_a^{BH}) - \alpha \delta(pK_a^{AH}) \quad (21)$$

which expresses the change in the rate constant of a proton transfer, AH + B⁻ → A⁻ + BH, when the pK_a values of both AH and BH are changing simultaneously. Note that in eq 20 we use the subscript "sol" to indicate that the changes in the equilibrium are induced by changes in the solvent rather than in the substituents (eq 21).

If one assumes that $\beta_{N,sol}$ and $\beta_{I,sol}$ are solvent independent one may estimate $\beta_{N,sol}$ and $\beta_{I,sol}$ by solving pairs of simultaneous equations of the type of eq 20. For example, for the change from water to 50% and from 50% to 70% Me₂SO the pair of simultaneous equations takes on the form

$$0 \rightarrow 50\% \quad 1.25 = 3.25\beta_{N,sol} - 0.75\beta_{I,sol} \quad (22)$$

$$50\% \rightarrow 70\% \quad 1.00 = 2.29\beta_{N,sol} - 0.38\beta_{I,sol} \quad (23)$$

from which we obtain $\beta_{N,sol} = 0.57$ and $\beta_{I,sol} = 0.80$. Choosing a different set, for example, the change from water to 50% Me₂SO, combined with that from 50% to 60% Me₂SO, leads to $\beta_{N,sol} = 0.59$, $\beta_{I,sol} = 0.89$; for the change from water to 50% Me₂SO, combined with the change from 60% to 70% Me₂SO, we obtain $\beta_{N,sol} = 0.56$, $\beta_{I,sol} = 0.76$.

It is important to realize that the reason why solving the pairs of simultaneous equations allows us to determine the $\beta_{N,sol}$ and $\beta_{I,sol}$ parameters is that the ratio $\log \gamma_{T-O}^D / \log \gamma_{CH(CN)_2}^D$ for one solvent change (e.g., for water to 50% Me₂SO, 3.25/0.75 = 4.53) is different from the ratio $\log \gamma_{T-O}^D / \log \gamma_{CH(CN)_2}^D$ for the other solvent change (e.g., for 50% to 70% Me₂SO, 2.29/0.38 = 6.03). In other words, it is because the dependence of the free energy of solvation of the oxanion not only shows a different *sensitivity* (slope) to the solvent composition from that of the malononitrile anion but because this dependence has a different *shape*.

The fact that the sets of $\beta_{I,sol}$ and $\beta_{N,sol}$ are quite consistent with each other, regardless of which combination of solvent changes (i.e., which set of simultaneous equations) is used, suggests that the assumption that these parameters are solvent independent is a reasonable approximation. The slight variations from one set to another is probably the result of several factors: (a) the solvent activity coefficients are only approximate; (b) there is some experimental uncertainty in the k_4 values;³⁴ (c) the assumption

(31) Watarai, H. *Bull. Chem. Jpn.* 1980, 53, 3019.

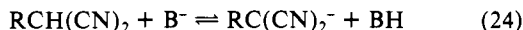
(32) The consistently somewhat higher $\delta \log K_4^D$ (eq 18) values compared to $\delta \log K_4^D$ (obsd) may indicate that $\log \gamma_{OH^-}^D$ slightly overestimates $\log \gamma_{T-O}^D$ because of a somewhat stronger hydrogen bonding solvation of the hydroxide ion. There may also be a slight contribution to the discrepancy from slightly positive $\log \gamma_{PhCHO}^D$ values and/or from slightly negative $\log \gamma_{CH_2(CN)_2}^D$ values; these latter would reduce $\log \gamma_{CH(CN)_2}^D$ (eq 19) thereby increasing $\delta \log K_4^D$ (eq 18).

(33) Note that the lower pK_a of malononitrile in the Me₂SO-containing solvents is not due to a stabilization of CH(CN)₂⁻, but to a stabilization of the hydrogen ion ($\log \gamma_{H^+}^D < 0$), which overcompensates the destabilization of CH(CN)₂⁻. By the same token, the increase in pK_a^{OH} is not as large as $\log \gamma_{T-O}^D$ because it is counteracted by the increased stability of the hydrogen ion.

of solvent independence of $\beta_{lg, sol}$ and $\beta_{N, sol}$ is only an approximation.

For these reasons we cannot attach great significance to the precise numerical values which are in the order of 0.78 ± 0.10 for $\beta_{lg, sol}$ and of 0.57 ± 0.05 for $\beta_{N, sol}$. We believe, however, that the inequality, $\beta_{lg, sol} > \beta_{N, sol}$, is authentic.³⁵ This inequality indicates that k_4 responds more strongly to the decreased solvation of $\text{CH}(\text{CN})_2^-$ (rate retarding) than to the decreased solvation of T^-_{O} (rate enhancing). The reason why the combination of the two effects nevertheless leads to a rate enhancement is that the decrease in the solvation of T^-_{O} ($\log {}^W\gamma_{\text{T}^-_{\text{O}}}$) is much larger than the decrease in the solvation of $\text{CH}(\text{CN})_2^-$ ($\log {}^W\gamma_{\text{CH}(\text{CN})_2^-}$).

Some insight into the meaning of this inequality or "imbalance"³⁶ may be gained by comparing our reaction with the deprotonation of malononitriles by oxyanions



Such a comparison suggests an analogy between $\beta_{lg, sol}$ and the Brønsted α obtained by varying R, and between $\beta_{N, sol}$ and the Brønsted β value determined by varying B^- . With carboxylate ions as bases, α and β were found to be virtually identical and close to unity,³⁷ i.e., no imbalance was observed.³⁸

On the basis of the results for reaction 24 one might have expected that $\beta_{lg, sol}$ and $\beta_{N, sol}$ should also be approximately equal to each other. However, $\beta_{N, sol}$ is significantly smaller than $\beta_{lg, sol}$. We attribute this to a reduction in $\beta_{N, sol}$ which is caused by the stronger solvation of the highly basic T^-_{O} oxyanion than that of a carboxylate ion.

Before attempting to explain how this stronger solvation may lead to a reduced $\beta_{N, sol}$ we would like to point out the similarity of this result with recent observations in the deprotonation of acetylacetone by hydroxide ion and carboxylate ions.⁴¹ In that system all rate constants for the deprotonation of acetylacetone were found to increase with increasing Me_2SO content of the solvent. However, this increase is relatively less for OH^- (e.g., 4.33-fold for the change from water to 50% Me_2SO) than with the carboxylate ions (e.g., 8.66-fold with acetate ion for the same solvent change), even though $\log {}^W\gamma_{\text{OH}^-} > \log {}^W\gamma_{\text{AcO}^-}$.³⁰ These observations are tantamount to a smaller β_{sol} for OH^- compared to acetate ion.

An alternative, but equivalent, way of looking at these proton-transfer data is to compare the Brønsted plots defined by the carboxylate ions in the two solvents and focus on the negative deviation of the hydroxide ion point from the Brønsted line. In water this deviation amounts to 2.79 log units, in 50% Me_2SO to more than 4.0 log units,⁴¹ again showing the stronger solvation effect for the hydroxide ion.

The reduced reactivity of hydroxide ion and of other strongly basic oxyanions relative to their $\text{p}K_a$ is a common observation.⁴² It has been attributed to the strong solvation of these ions, coupled with the requirement that the partial desolvation which accompanies the reaction is ahead of bond formation in the transition state.⁴³ The small $\beta_{N, sol}$ for the breakdown reaction of T^-_{O} as well as the small β_{sol} in the deprotonation of acetylacetone by OH^- (or the stronger negative deviation of the OH^- point from the

Brønsted plot in Me_2SO -water)⁴¹ indicate that this effect is magnified in the Me_2SO -containing solvents. In other words, the energy required for the partial desolvation of the strongly basic alkoxide ions seems to be even larger in Me_2SO -water than in water.

This conclusion may seem paradoxical since in the Me_2SO -water mixtures solvation of the oxyanion is weaker than in water.⁸ In view of our still very incomplete understanding of the molecular mechanism of solvation, particularly in mixed solvents,⁴⁴ any attempts to explain this apparent paradox must remain crude and tentative at best. Nevertheless, it is helpful to examine a number of simple solvation models which might provide a qualitative insight.

The crudest solvation model would be one where all solvation effects are accounted for by the inner solvation shell. In such a model there may be n water molecules around the anion in water, while in Me_2SO -water one (or more) of the water molecules may be replaced by a Me_2SO molecule. Partial desolvation of the anion in Me_2SO -water should then be easier than in water since it would presumably involve the removal of a Me_2SO molecule which is a weaker solvator than water.⁸ This model can therefore not account for the experimental observations.

From the above discussion it appears that a successful model would have to include effects from the secondary solvation shell. In one version of such a model it is assumed that even in Me_2SO -water mixtures the inner solvation shell of the ion contains only water molecules because of the presumably greater affinity of the hydrogen-bonding water molecules to the anion.⁸ The reduced overall solvation of the ion would then mainly be a consequence of weaker solvation beyond the inner sphere.

A perhaps more realistic version of this model is the one suggested by Kebarle et al.⁴⁵ According to results in the gas phase it appears that the reason why liquid Me_2SO is a poorer solvator of anions (at least of halide ions) than liquid water is not so much because the solvation energy of a Me_2SO molecule interacting with the ion is smaller than that of a water molecule (it is in fact larger in the gas phase⁴⁵) but because of the large size of the inner solvation cluster $\text{B}^-(\text{Me}_2\text{SO})_n$. This large size prevents solvation beyond the inner sphere of $\text{B}^-(\text{Me}_2\text{SO})_n$ while such solvation is quite effective with the smaller $\text{B}^-(\text{H}_2\text{O})_n$.⁴⁶

Regardless of which version of this model is preferred, it is relatively easy to visualize why the removal of a solvent molecule from the inner solvation shell would be more difficult in Me_2SO -water than in water. It may simply be a matter of the ion being less able to shed a solvent molecule when it is already inherently less stable by virtue of being placed in a less-solvating medium. In other words, the weaker the solvation of the ion, the more energy it takes to remove a solvent molecule.⁴⁷ This situation is similar to observations in the gas phase where the sequential removal of solvent molecules from the solvation shell of an ion becomes increasingly more difficult the fewer solvent molecules are left behind,^{45,48} i.e., $\text{B}^-(\text{sol})_{n-1} \rightarrow \text{B}^-(\text{sol})_{n-2} + \text{sol}$ is more difficult than $\text{B}^-(\text{sol})_n \rightarrow \text{B}^-(\text{sol})_{n-1} + \text{sol}$, even though $\text{B}^-(\text{sol})_{n-1}$ is of higher energy than $\text{B}^-(\text{sol})_n$.

Mechanism of the $k_{34}^{\text{H}_2\text{O}}$ Step. The direct breakdown of T^-_{O} into benzaldehyde and malononitrile becomes dominant in strongly acidic solution. A similar direct breakdown has been observed in the hydrolysis of 1,1-dinitro-2,2-diphenylethylene⁴ and arylidene Meldrum's acids.² In past discussions^{1,2,4} we have favored a

(34) The uncertainty in the absolute values of k_4 may well amount to factors of two or three. However, most of these uncertainties tend to cancel in $\delta \log {}^Wk_4^{\text{D}}$ because the systematic errors in our estimates should be largely the same in all solvents.

(35) The inequality $\beta_{lg, sol} > \beta_{N, sol}$ also remains if somewhat lower $\log {}^W\gamma_{\text{T}^-_{\text{O}}}$ values are assumed which may be justified since $\delta \log {}^Wk_4^{\text{D}}$ (obsd) $< \delta \log {}^Wk_4^{\text{D}}$ (eq 18).

(36) Jencks, D. A.; Jencks, W. P. *J. Am. Chem. Soc.* **1977**, *99*, 7948.

(37) Bell, R. P.; Grainger, S. J. *Chem. Soc., Perkin Trans. 2* **1976**, 1367.

(38) This contrasts with the deprotonation of nitroalkanes,³⁹ ketoesters,³⁷ and arylacetoneitriles⁴⁰ where strong imbalances have been observed.

(39) (a) Fukuyama, M.; Flanagan, P. W. K.; Williams, F. T., Jr.; Frainer, L.; Miller, S. A.; Schechter, H. *J. Am. Chem. Soc.* **1970**, *92*, 4689. (b) Bordwell, F. G.; Boyle, W. J., Jr. *Ibid.* **1972**, *94*, 3907. (c) Bordwell, F. G.; Bartmess, J. E.; Hautala, J. A. *J. Org. Chem.* **1978**, *43*, 3107. (d) Kresge, A. J. *Can. J. Chem.* **1975**, *52*, 1897.

(40) Bernasconi, C. F.; Hibdon, S. A. *J. Am. Chem. Soc.* **1983**, *105*, 4343.

(41) Bernasconi, C. F.; Bunnell, R. D. *Isr. J. Chem.*, in press.

(42) Kresge, A. J. *Chem. Soc. Rev.* **1973**, *2*, 475.

(43) Jencks, W. P.; Brant, S. R.; Gandler, J. R.; Fendrich, G.; Nakamura, C. *J. Am. Chem. Soc.* **1982**, *104*, 7045 and references cited therein.

(44) Reichardt, C. "Solvent Effects in Organic Chemistry"; Verlag Chemie: New York, 1979.

(45) Magnera, T. F.; Caldwell, G.; Sunner, J.; Ikuta, S.; Kebarle, P. *J. Am. Chem. Soc.* **1984**, *106*, 6140.

(46) Other authors, based on different kinds of evidence, have also concluded that the superior solvation of anions in liquid water is due as much to cooperative effects beyond the inner shell as to specific coordination effects: (a) Cogley, D. R.; Butler, J. N.; Grunwald, E. *J. Phys. Chem.* **1971**, *75*, 1477. (b) Arnett, E. M.; Chawla, B.; Hornung, N. J. *J. Sol. Chem.* **1977**, *6*, 781.

(47) Note that this model still allows for the ion to be more reactive in the mixed solvent because the extra activation energy required for its desolvation is overcompensated by its greater destabilization brought about by the transfer from water to Me_2SO -water.

(48) (a) Kebarle, P. *Annu. Rev. Phys. Chem.* **1977**, *28*, 445. (b) Lan, Y. K.; Ikuta, S.; Kebarle, P. *J. Am. Chem. Soc.* **1982**, *104*, 1462.

